Function of the [2Fe−2S] Cluster in Mammalian Ferrochelatase: A Possible Role as a Nitric Oxide Sensor†

Vera M. Sellers,‡ Michael K. Johnson,§ and Harry A. Dailey*,‡

Departments of Microbiology and Chemistry and Center for Metalloenzyme Studies, University of Georgia, Athens, Georgia 30602

Received November 6, 1995; Revised Manuscript Received December 21, 1995⊗

ABSTRACT: Ferrochelatase (E.C. 4.99.1.1) is the terminal enzyme of the heme biosynthetic pathway, catalyzing the insertion of ferrous iron into protoporphyrin. In mammals the enzyme contains a labile [2Fe−2S] center. Although this cluster is absent in all prokaryotic, plant, and yeast ferrochelatases, its destruction or elimination from the mammalian enzyme results in loss of enzyme activity. In the current study we present data which clearly demonstrate that mammalian ferrochelatase is strongly inhibited by nitric oxide and that this effect is mediated via destruction of the [2Fe−2S] cluster. Carbon monoxide has no inhibitory effect, and yeast ferrochelatase, which lacks the [2Fe−2S] cluster, is not affected by NO (or CO). EPR and UV−visible absorption of purified recombinant human ferrochelatase provides evidence that NO is targeting the [2Fe−2S] center. UV−visible absorption spectroscopy of both human and murine recombinant ferrochelatase incubated with NO or the NO donor, *S*-nitroso-*N*-acetylpenicillamine (SNAP), indicate a rapid loss of the visible absorption spectrum of the [2Fe−2S] cluster. EPR studies of the resulting samples reveal the characteristic axial $S = {}^1/_2$ resonance, $g_\perp = 2.033$, and $g_\parallel = 2.014$ of a cysteinyl-coordinated monomeric iron−dinitrosyl cluster degradation product. Parallel spectroscopic studies of spinach ferredoxin, which also contains a [2Fe−2S] cluster, gave no indication of NO-induced cluster degradation under the same experimental conditions. Exposure of DMSO-induced murine erythroleukemia cells exposed to SNAP results in an initial decrease in heme production, suggesting that *in vivo* the cluster is rapidly destroyed. The potential physiological relevance of these data to the anemias that are found in individuals with chronic infections is discussed.

Mammalian ferrochelatase (protoheme lyase, E.C. 4.99.1.1), the terminal enzyme of the heme biosynthetic pathway, catalyzes the insertion of ferrous iron into the protoporphyrin IX macrocycle to form heme (Dailey, 1990). Ferrochelatase, which is nuclear encoded, is synthesized in the cytoplasm and translocated into the mitochondrion where the enzyme is proteolytically processed to its mature size of 42 kDa (Karr & Dailey, 1988; Camadro & Labbe, 1988). The enzyme is bound to the inner mitochondrial membrane with the active site facing the mitochondrial matrix (Harbin & Dailey, 1985; Jones & Jones, 1969). Recently it was demonstrated that human (Dailey et al., 1994a) and mouse (Ferreira et al., 1994) ferrochelatases contain [2Fe−2S] metal centers. The putative [2Fe−2S] binding region contains a [Cys-X_7-Cys-X_2-Cys-X_4-Cys] motif in the carboxyl-terminal region of the mammalian enzyme (Dailey et al., 1994a). Yeast and plant ferrochelatases do not contain this motif, and the bacterial ferrochelatase altogether lacks the final 30 amino acid residues at the carboxyl-terminus. Interestingly, an engineered recombinant human ferrochelatase which is truncated 30 residues from the carboxyl terminus does not contain the cluster and has no enzyme activity (Dailey et al., 1994a).

The properties of the $[2Fe-2S]^{2+,+}$ cluster in recombinant mammalian ferrochelatases are very similar to those found in 2Fe ferredoxins, as judged by variable-temperature MCD,[1] Mössbauer, and EPR studies (Dailey et al., 1994a; Ferreira et al., 1994). However, no redox role has been found for the cluster in ferrochelatase. The iron−sulfur cluster is distinct from the ferrous iron substrate binding region (Dailey et al., 1994a), and the cluster does not appear to play any role in the reduction of ferric iron to ferrous iron. While the presence of the cluster is required for enzyme activity (Dailey et al., 1994a), a specific role has remained elusive. Here we present results that are consistent with a regulatory role for the cluster as a nitric oxide sensor. This raises the possibility that NO-induced inactivation of mammalian ferrochelatase via cluster degradation may be a defense mechanism against bacterial infection.

MATERIALS AND METHODS

Purification of Ferrochelatase. Recombinant human, murine, and yeast ferrochelatase were produced in *Escherichia coli* JM109 as previously described (Dailey et al., 1994a,b). Human murine, and yeast ferrochelatase were expressed using a tac promoter vector and purified with slight modifications to the previous method (Dailey et al., 1994b). Sodium dithionite (1 mM) was added to all solutions

† This work was supported by grants from the National Institutes of Health (DK32303 and DK35898 to H.A.D. and GM51962 to M.K.J.) and by the National Science Foundation Research Training Group Award to the Center for Metalloenzyme Studies (DIR9014281).

* Address correspondence to this author. Tel: (706) 542-2690. FAX: (706) 542-2674. E-mail: dailey@bscr.uga.edu.

‡ Department of Microbiology.

§ Department of Chemistry.

⊗ Abstract published in *Advance ACS Abstracts,* February 15, 1996.

[1] Abbreviations: SNAP, *S*-nitroso-*N*-acetylpenicillamine; SIN-1, 3-morpholinosydnonimine; DTT, dithiothreitol; MCD, magnetic circular dichroism; MEL, murine erythroleukemia; IRP, iron regulatory protein.

0006-2960/96/0435-2699$12.00/0 © 1996 American Chemical Society

excluding the final elution from the HiTrap Blue Sepharose affinity column. The modification was the inclusion of passage of the detergent-solubilized fraction through a DEAE Sepharose column, equilibrated with the solubilization buffer (Dailey et al., 1994b) prior to the HiTrap blue column. This additional step removed the traces of enzyme bound heme and porphyrin that were present in earlier preparations which interfered with MCD and visible spectroscopy. Purified spinach ferredoxin was a gift from Prof. David Knaff (Texas Tech University).

Ferrochelatase Assays. Ferrochelatase activity was assayed anaerobically using the pyridine hemachromagen assay (Dailey & Fleming, 1983). For assays in which NO was present, an NO-saturated solution in 0.1 M Tris MOPS, pH 8.1, was added to anaerobic, sealed assay tubes in increasing amounts and brought to a final volume of 500 μL with degassed 0.1 M Tris MOPS, pH 8.1. A total of 0.1 nmol of human or yeast ferrochelatase in a volume of 100 μL of elution buffer was incubated in the NO equilibrated buffer for 1 h. Using anaerobic solutions, the assay mixture was made 0.1 μM in ferrous ammonium sulfate, 0.1 μM in protoporphyrin IX (Porphyrin Products, Logan, UT), 5 mM in β-mercaptoethanol, and 0.1 M in sodium bicarbonate. Following incubation at 37 °C for 30 min, the sealed tubes were opened, reactions were stopped, and product was quantified as previously described (Dailey & Fleming, 1983). The above procedures were also followed substituting carbon monoxide for nitric oxide. Anaerobic assays were also performed after incubating 0.1 nmol purified human ferrochelatase with the NO donor, SNAP (Alexis Corp., San Diego, CA; Field et al., 1978), 0.1−1.0 mM final concentration, for 1 h, and after incubation of ferrochelatase with both superoxide dismutase, 25 mM, (Sigma) and SNAP, 0.1−1.0 mM, for 1 h. Protein quantification and measurement of product from the pyridine hemochromagen assay were performed with a Varian 219 dual-beam spectrophotometer.

UV−Visible Absorption Spectroscopy. To quantitate loss of the [2Fe−2S] cluster following addition of the NO donor, SNAP, UV−Visible absorption studies of recombinant human ferrochelatase, 1 μM, and purified spinach ferredoxin, 3 μM, in 1.0 mL of elution buffer (20 mM Tris MOPS, pH 8.1, 20% glycerol, 1% sodium cholate, 1.5 M KCl, 10 μg of phenylmethylsulfonyl fluoride/mL, 2 mM DTT), were carried out using a Shimadzu 3100PC dual-beam spectrophotometer. Following an initial scan, SNAP (in DMSO, final concentration 0.1% wt/vol) was added to the sample and to reference cuvettes to yield a final concentration of 0.2 mM. Repetitive scans were run anaerobically (620−240 nm) at 5 min intervals to monitor loss of cluster absorption.

EPR Spectroscopy. EPR samples of NO-treated human ferrochelatase, 3 μM, were prepared under anaerobic conditions using NO-saturated 0.1 M Tris MOPS, pH 8.1. The final sample contained 50% volume of the NO-saturated buffer. The EPR tubes were transferred from an anaerobic chamber and immediately frozen in liquid nitrogen. The samples used for UV−visible spectroscopy, spinach ferredoxin incubated with 0.2 mM SNAP for 72 h at 4 °C and human ferrochelatase incubated with 0.2 mM SNAP for 1 h at 23 °C, were also frozen in EPR tubes. EPR spectra were recorded using a Bruker ESP-300E spectrometer equipped with an Oxford ESR9 cryostat.

Cell Culture. Murine erythroleukemia cells were cultured in α-MEM medium supplemented with 7% fetal bovine serum as described previously (Conder et al., 1991). Erythroid differentiation was induced by addition of 2% DMSO. At the times indicated, 0.5 μM SNAP was added to cultures and after 30 min, cells were then pelleted, washed with α-MEM medium at 37 °C, and resuspended in their original volume with fresh α-MEM and 2% DMSO.

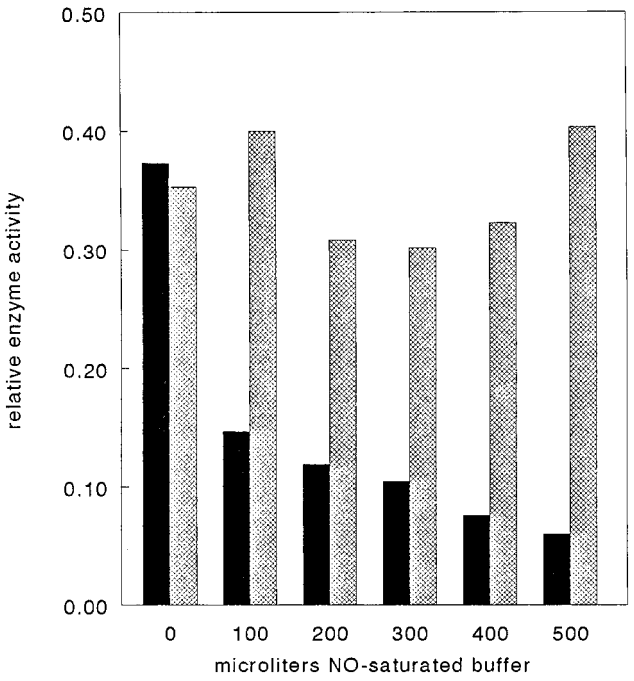

FIGURE 1: Effect of NO on ferrochelatase activity. Purified recombinant human (solid bars) and yeast (hatched bars) ferrochelatase were exposed to the indicated amounts of a NO-saturated buffer for 1 h at 23 °C. Anaerobic assays were performed as described in Materials and Methods. This experiment was repeated three times, resulting in data with less than 10% standard deviation.

Heme Assays. Heme was quantified following conversion to protoporphyrin using the oxalic acid method previously described (Sassa et al., 1978). Fluorescence was quantitated with a Perkin-Elmer 650-40 fluorimetric spectrophotometer (405 nm excitation, 635 nm emission).

RESULTS

Enzyme Activity. The effect of NO on the activity of purified recombinant human ferrochelatase was investigated by exposing the enzyme to increasing amounts of an NO-saturated buffered solution for 1 h. Both mammalian ferrochelatase, which contains a [2Fe−2S] cluster, and yeast ferrochelatase, which does not contain the [2Fe−2S] cluster, were examined. In all experiments, care was taken to maintain anaerobic conditions and to monitor pH, since O_2 can react with NO resulting in acidification of the solution. Although it was not possible to monitor the exact concentration of NO in the assay mixture, the addition of increasing amounts of NO to human ferrochelatase clearly result in corresponding decreases in enzyme activity as shown in Figure 1. Yeast ferrochelatase under the same conditions was unaffected within experimental error.

In addition to NO, CO was also examined since it has been shown to interact with certain iron-containing proteins. When the above procedures are repeated substituting CO saturated buffer for the NO-saturated buffer, the activities of both human and yeast ferrochelatases remain constant. In similar anaerobic assays, first incubating human ferro-

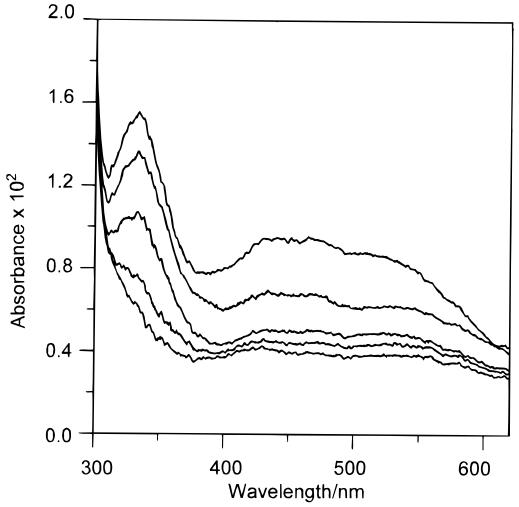

FIGURE 2: Time dependence of the effect of SNAP on the UV−visible absorption spectra of recombinant human ferrochelatase. Spectra were recorded 0, 30, 60, 90, and 120 min after addition of a 200-fold stoichiometric excess of SNAP. Absorption at all wavelengths decreases with increased length of exposure to SNAP. Experimental details are described in Materials and Methods.

chelatase with the NO donor SNAP, enzyme activity correspondingly decreases as with the NO-saturated buffer. When superoxide dismutase is included to remove superoxide and, effectively, peroxynitrite, followed by addition of increasing concentrations of SNAP, superoxide dismutase does not eliminate any inhibitory effect of SNAP on human ferrochelatase.

UV−Visible Absorption. The visible absorption spectrum of human recombinant ferrochelatases in the 300−600 nm region is shown in Figure 2. It is very similar to the published spectrum (Dailey et al. 1994a), except that the samples used in this work contained none of the heme impurity as evidenced by the absence of a pronounced Soret band at 420 nm. The absence of heme impurity in these samples was also confirmed by variable temperature MCD studies of oxidized and dithionite-reduced samples (data not shown). Since the visible absorption in this spectral region arises exclusively from the $[2Fe-2S]^{2+}$ center, it provides a convenient and direct monitor of NO-induced cluster degradation. Figure 2 shows that the cluster is degraded over a period of 2 h when human ferrochelatase, 1 μM, is exposed to 0.2 mM SNAP. Parallel control experiments under identical conditions using spinach ferredoxin with SNAP and human ferrochelatase without addition of SNAP showed no change in absorption over this time period. Hence the cluster degradation is attributed directly to the presence of SNAP and the [2Fe−2S] cluster in human ferrochelatase is clearly far more sensitive than those in plant type ferredoxins to SNAP-induced degradation. In the absence of 0.2 mM DTT, addition of SNAP resulted in precipitation of the human ferrochelatase from solution and this effect was enhanced at high enzyme concentrations. No such precipitation was observed in parallel experiments with yeast ferrochelatase in the absence of DTT. Since yeast ferrochelatase does not contain a [2Fe−2S] cluster, it seems likely that enzyme precipitation in the absence of DTT is a direct result of cluster degradation. This line of argument, therefore, provides additional evidence that the cluster is the sole target for SNAP in human ferrochelatase.

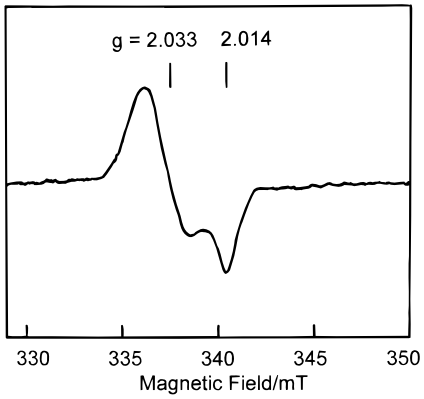

FIGURE 3: EPR spectrum of NO-treated recombinant human ferrochelatase. Human ferrochelatase (500 μL, 6 μM) was treated anaerobically with 500 μL of a buffered saturated NO solution and frozen immediately. EPR conditions: microwave frequency, 9.60 GHz; modulation amplitude, 0.64 mT; microwave power, 1 mW; temperature, 35 K.

EPR Spectroscopy. Direct evidence that NO was responsible for cluster degradation in samples of human ferrochelatase treated with NO or SNAP came from EPR spectroscopy. Purified human ferrochelatase exhibits no EPR signals, in accord with the presence of an $S = 0$ $[2Fe-2S]^{2+}$ cluster. Anaerobic addition of sodium dithionite effects cluster reduction, and the resulting samples exhibit the characteristic $g = 2.002$, 1.936, and 1.912 resonances associated with the $S = {}^1/_2[Fe-2S]^+$ cluster (Dailey et al., 1994a). Both as prepared and dithionite-reduced samples of human ferrochelatase, in the absence of DTT, exhibited the same axial $S = {}^1/_2$ EPR signal, $g_\perp = 2.033$ and $g_\parallel = 2.014$, when treated with a NO-saturated buffer solution, see Figure 3. The same resonance was also observed, albeit weaker due to the lower enzyme concentration, for the samples used in the UV−visible absorption studies after treatment for 2 h with 0.2 mM SNAP (data not shown). Nitric oxide has been shown to react intracellularly and *in vitro* with several iron−sulfur and other iron-containing proteins to give characteristic EPR signals (Drapier et al., 1991; Lepoivre et al., 1994; Lee et al., 1994). The resonance observed for NO-treated human ferrochelatase is identical to that observed for other NO-treated iron−sulfur proteins and is attributed to a monomeric cysteinyl-coordinated iron−dinitrosyl complex which appears to be the product of NO-induced cluster degradation (Butler et al., 1988; Drapier et al., 1991; Lee et al., 1994). In the absence of exogenous Fe^{2+}, this signal was not observed in sampls of recombinant yeast ferrochelatase after treatment with NO under identical conditions.

MEL Cell Exposure to SNAP. Murine erythroleukemia cells are virus-transformed erythroid precursor cells, which are induced to erythroid differentiation by addition of DMSO or other compounds. Following induction with 2% DMSO, ferrochelatase increases gradually over 96 h (Condor et al., 1991). DMSO-induced cultures were incubated with low concentrations of SNAP to produce 30 min pulses of NO after 6, 12, 24, and 48 h. SNAP treatment at 6 and 12 h had little effect on the production of heme, whereas treatment at 24 or 48 h resulted in a significant delay in heme production. Such data are consistent with a rapid inactivation of ferrochelatase by NO which then results in a decreased ability to synthesize heme. A lack of effect at the 6 and 12 h pulse reflects the fact that ferrochelatase levels are low at that time. The pulse at 24 h results in a delay in heme

synthesis, suggesting that NO treatment effectively destroys whatever ferrochelatase may be present at 24 h and, thereby, retards heme synthesis.

DISCUSSION

Recently it has been shown that ferrochelatase activity decreased in cultured rat hepatocytes treated with the NO-generating compound SNAP (Kim et al., 1995) and in a cultured macrophage cell line treated with interferon-γ and lipopolysaccharide to induce endogenous NO production (Furukawa et al., 1995). In the case of the macrophage cell line, this decrease in activity was not attributable to a decrease in immunoreactive ferrochelatase protein. Both sets of researchers suggested that the observed effect of NO on ferrochelatase may be mediated via the [2Fe−2S] cluster, but neither presented compelling data on the purified enzyme to support this suggestion. The suggestion that the [2Fe−2S] cluster was involved in the NO response is an interesting hypothesis, but the lack of a previously characterized eukaryotic [2Fe−2S] cluster that had been shown to be sensitive to NO along with the fact that the product, protoheme, and one substrate, ferrous iron of ferrochelatase have, themselves, been shown to react with NO in other proteins, raised questions that could be answered experimentally.

The data that we present above clearly demonstrate that NO rapidly and effectively causes disassembly of the [2Fe−2S] cluster of mammalian ferrochelatases. Loss of the cluster results in concomitant loss of enzyme activity. Spinach ferredoxin, which also contains a [2Fe−2S] cluster, is unaffected under the same conditions that result in loss of the ferrochelatase cluster. Yeast ferrochelatase, which does not contain a [2Fe−2S] cluster is also unaffected by NO. Thus, NO is not inactivating ferrochelatase via interaction with an enzyme−substrate, an enzyme−product complex, or a protein cysteinyl or tyrosyl residue but is reacting directly with the cluster. Neither the mammalian or the yeast enzyme is affected by CO.

Furukawa and co-workers (1995) reported that incubation of purified ferrochelatase, which contained less than stoichiometric amounts of the cluster and some residual heme or porphyrin, with 0.1−1.0 mM SIN-1 resulted in the loss of enzyme activity and the disappearance of the characteristic iron−sulfur absorption spectrum of mammalian ferrochelatase. The utilization of SIN-1, which is known to generate superoxide, hydroxyl radicals, and other potent oxidants in addition to NO (Gergel et al., 1995), and the lack of EPR evidence for a iron−nitrosyl species leaves open the possibility that an agent other than NO was responsible for the observed effects. Interestingly, they also reported a loss of activity by *E. coli* ferrochelatase (which lacks a cluster) that would suggest the observed inactivation was attributable to an oxidant acting at a different site and not a specific NO-cluster interaction. In the current study we have used NO gas and SNAP as an NO generator. The concentrations of SNAP used herein are lower than those used by others in crude cell extracts (Furukawa et al., 1995), and all of the current data were gathered on purified human ferrochelatase containing a stoichiometric amount of the cluster and without the presence of contaminating heme. Additionally, our data show that superoxide dismutase does not inhibit SNAP inactivation of human ferrochelatase and thereby suggest that superoxide and peroxynitrite are not the effective agents.

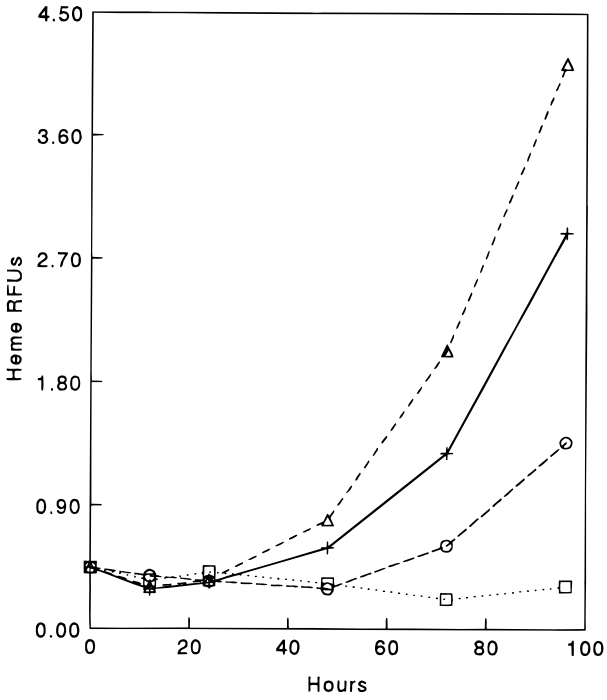

FIGURE 4: Effect of SNAP on heme production in differentiating MEL cells. Following induction with DMSO, MEL cells were pulsed for 30 min with 5 μM SNAP at 6 (△), 12 (+), 24 (○), and 48 h (□). For each set, heme assays were performed at 0, 12, 24, 48, 72, and 96 h as described in Materials and Methods. Values are shown as relative fluorescence units (RFU) per 5×10^6 cells.

The currently known ferrochelatase sequences include a variety of prokaryotic and plant enzymes, the yeast enzyme, and mouse, bovine, and human ferrochelatases (Dailey, 1990; Nakahashi et al, 1990; Taketani et al., 1990; Labbe-Bois, 1990; Brenner & Fraiser, 1991; Hansson & Hederstedt, 1992; Frustaci & O'Brian, 1992; Miyamoto et al., 1991, 1994; Smith et al., 1994). Among these only the mammalian enzymes contain the four cysteines in the 30-residue carboxyl-terminal region that are essential for assembly of the [2Fe−2S] cluster (Dailey et al., 1994a), see Figure 5. That the cluster is not essential for actual catalysis is demonstrated by the fact that it is not present in nonmammalian enzymes. However, in those enzymes which contain the cluster, loss of the cluster clearly correlates with loss of enzyme activity. The fact that the cluster is quite labile and responsive to NO suggests that this feature may serve as a functional on/off switch for the enzyme activity, perhaps by inducing a structural alteration. The observation that spinach ferredoxin, which also has a [2Fe−2S] cluster, is not affected by NO suggests that the mammalian ferrochelatase cluster is distinct and that the observed NO response is not a general property of all biological [2Fe−2S] clusters.

The *E. coli* SoxR protein contains a [2Fe−2S] cluster that is sensitive to NO and oxidizing agents (Nunoshiba et al., 1993; Hildago et al., 1995). The SoxR cluster, however, is structurally quite distinct from all other [2Fe−2S] clusters in that it has only a single residue between the two internal cys residues rather than the usual C-X-X-C spacing (Hildago et al., 1995), see Figure 5. Interestingly the closest sequence match to the SoxR cluster containing region is found in the [4Fe−4S] clusters of thermophilic bacteria such as *Thermatoga maritima* (Darimont & Sterner, 1994).

The explanation for why the mammalian ferrochelatase [2Fe−2S] cluster is so readily destroyed by low NO

Human Fc	N	E	L	C	S	K	Q	L	T	L	S	C	P	L	C	V	N	P	V	-	C	R	E
Mouse Fc	N	K	L	C	S	T	Q	L	S	L	N	C	P	L	C	V	N	P	V	-	C	R	K
Bovine Fc	N	E	R	C	S	T	Q	L	T	L	S	C	P	L	C	V	N	P	T	-	C	R	E
S. oleracea. Fd	P	Y	S	C	R	A	-	-	-	G	S	C	S	S	C	A	G	X_{25}	L	T	C	A	A
E. coli SoxR	L	D	G	C	I	G	-	-	-	-	-	C	G	-	C	L	S	R	S	D	C	P	L
T. maritima Fd	A	D	A	C	I	G	-	-	-	-	-	C	G	V	C	E	N	L	-	-	C	P	D

FIGURE 5: Comparison of sequence of mammalian ferrochelatases with selected iron−sulfur proteins in the region of coordinating cysteine residues. Dashes indicate breaks in the sequences to facilitate alignment. Shown are sequences for human (Nakahashi et al., 1990), mouse (Taketani et al., 1990), and bovine (Brenner & Frasier, 1991) ferrochelatase, *S. oleracea* ferredoxin (Takahashi et al., 1983) *E. coli* SoxR (Amábile-Cuevas & Demple, 1991), and *T. maritima* ferredoxin (Darimont & Sterner, (1994). The cys residues proposed to be involved in cluster coordination are underlined. The sequence shown for *T. maritima* is a portion of a sequence involved in coordination of [4Fe−4S] clusters.

concentrations while the plant ferredoxin cluster is not may reside in the physical spacing of the coordinating cysteine residues as well as the nature of adjacent residue side chains. Ferrochelatase has a C-X_7-C-X_2-C-X_4-C arrangement while plant ferredoxins have a C-X_4-C-X_2-C-X_{29}-C arrangement of coordinating cysteins. Interesting, preliminary experiments conducted in this laboratory suggest that mouse and human ferrochelatase may have slightly different sensitivities to NO (data not shown). These two proteins differ significantly at two residues (E to K, and K to T) in the cluster region, and this may contribute to this stability of the cluster.

When examined in isolation, this NO response may seem without logic, but when examined in the complete context of iron transport, utilization, and storage in mammals, an explanation, based upon previous clinical data seen in chronic infection and some malignant disorders becomes apparent. During such states of chronic inflammation, nitric oxide is produced by macrophages and other cells by an inducible nitric oxide synthase (iNOS) (Nussler & Billiar, 1993). Bacterial lipopolysaccharide and cytokines, such as interferon-γ and tumor necrosis factor-α, activate the inducible form of nitric oxide synthase to generate large amounts of nitric oxide throughout the life of the enzyme. By direct bacteriocidal activity, as well as by targeting specific proteins, NO plays an important part in the mammalian immune mechanism. In addition, NO from iNOS has recently been shown to directly mediate iron regulation during chronic inflammation (Weiss et al., 1994).

It has been proposed that nitric oxide from iNOS indirectly controls levels of ferritin and transferrin receptor expression through activation of the iron regulatory protein (IRP). Transferrin receptor mRNA stabilized by IRP results in an increase of transferrin receptor protein on the cell surface (Pantopoulos & Hentze, 1995; Oria et al., 1995), which in turn leads to an increased clearance of iron from the serum. Although ferritin mRNA translation has been suggested to be inhibited by IRP, some groups have documented an overall increase of cellular ferritin concentrations (Pantopoulos & Hentze, 1995; Oria et al., 1995), leading to sequestration of cellular iron in ferritin. Additionally, heme oxygenase, which is responsible for the breakdown of free heme and release of iron, appears to be induced by NO (Kim et al., 1995). Since ferrochelatase is inactivated by NO, any iron released from heme degradation is then also accumulated by intracellular ferritin. Thus, this entire response to NO serves to decrease cellular free heme levels and to sequester both serum and cellular iron into ferritin (Scheme 1).

It is well-known that the availibility of iron to invading microorganisms can determine the success or failure of an infection (Weinberg, 1971). In addition, for many pathogenic microorganisms, iron from heme is an obligatory requirement for growth (Smith, 1990). The binding of both iron and heme by host serum proteins has long been recognized as part of the host immune response. Thus a decrease in heme production through the inactivation of ferrochelatase would serve to limit heme availability for pathogens. Additionally, the observation of anemia in individuals with chronic inflammation may be explained by the persistent inhibition of erythroid precursor ferrochelatase during long-term infection. Additional support for this explanation comes from the data of differentiating erythroid cells where the inhibition of ferrochelatase by NO results in an immediate reduction of heme synthesis. Thus it is possible that inhibition of ferrochelatase alone, *in vivo*, could result in anemia during chronic infections.

In conclusion we have clearly shown that the mammalian ferrochelatase is rapidly inactivated by low concentrations of NO and that this inactivation is mediated via destruction of the [2Fe−2S] cluster. The potential physiological role of this regulation of the enzyme by NO may be as a component of the overall regulation of iron metabolism during infection.

Scheme 1: Model for the Role of Ferrochelatase in the Mammalian Immune Response[a]

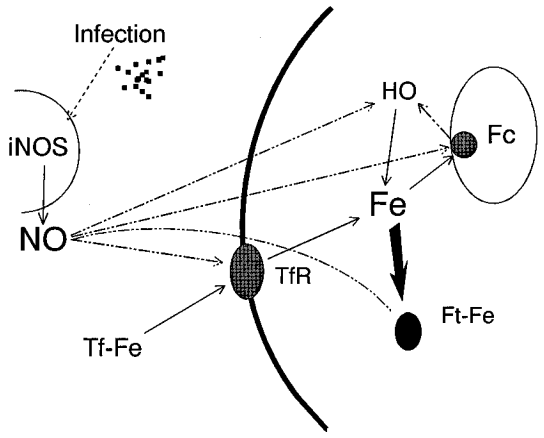

[a] An initial infection stimulates the macrophage to an activated state. The macrophage inducible nitric oxide synthase (iNOS) then releases nitric oxide. NO, a small membrane permeable molecule, freely enters the cell, causing an increase of transferrin receptor (TfR) on the cell surface. Intracellular ferritin (Ft−Fe) levels also increase. NO mediates an elevation of heme oxygenase (HO) mRNA and a decrease in ferrochelatase (Fc) activity. The overall effects are decreased serum transferrin bound iron (Tf−Fe), decreased cellular heme synthesis, and increased iron storage in ferritin. Thereby follow the decrease in cellular heme levels and the reduction of the iron source for the pathogen.

REFERENCES

Amábile-Cuevas, C. F., & Demple, B. (1991) *Nucleic Acids Res. 19*, 4479−4484.

Brenner, D. A., & Frasier, F. (1991) *Proc. Natl. Acad. Sci. U.S.A. 88*, 849−853.

Butler, A. R.; Glidewell, C., & Li, M.-H. (1988) *Adv. Inorg. Chem. 32*, 335−393.

Camadro, J.-M., & Labbe, P. (1988) *J. Biol. Chem. 263*, 11675−11682.

Conder, L. H., Woodard, S. I., & Dailey, H. A. (1991) *Biochem. J. 275*, 321−326.

Dailey, H. A. (1990) in *Biosynthesis of Heme and Chlorophylls* (Dailey, H. A., Ed.) pp 123−161, McGraw-Hill, New York.

Dailey, H. A., & Fleming, J. E. (1983) *J. Biol. Chem. 258*, 11453−11459.

Dailey, H. A., Finnegan, M. G., & Johnson, M. K. (1994a) *Biochemistry 33*, 403−407.

Dailey, H. A., Sellers, V. M., & Dailey, T. A. (1994b) *J. Biol. Chem. 269*, 390−395.

Darimont, B., & Sterner, R. (1994) *EMBO J. 13*, 1772−1781.

Drapier, J.-C., Pellat, C., & Henry, Y. (1991) *J. Biol. Chem. 266*, 10162−10167.

Ferreira, G. C., Franco, R., Lloyd, S. G., Pereira, A. S., Moura, I., Moura, J. J. G., & Huynh, B. H. (1994) *J. Biol. Chem. 269*, 7062−7065.

Field, L., Dilts, R. V., Ravichandran, R., Lenhert, P. G., & Carnahan, G. E. (1978) *J. Chem. Soc., Chem. Commun.* 249−250.

Frustaci, J. M., & O'Brian, M. (1992) *J. Bacteriol. 174*, 4223−4229.

Furukawa, T., Kohno, H., Tokunaga, R., & Taketani, S. (1995) *Biochem. J. 310*, 533−538.

Gergel, D., Milik, V., Ondria, K., & Cederbaum, A. I. (1995) *J. Biol. Chem. 270*, 20922−20929.

Hansson, M., & Hederstedt, L. (1992) *J. Bacteriol. 174*, 8081−8093.

Harbin, B. M., & Dailey, H. A. (1985) *Biochemistry 24*, 366−370.

Hildago, E., Bollinger, J. M., Jr., Bradley, T. M., Walsh, C. T., & Demple, B. (1995) *J. Biol. Chem. 270*, 20908−20914.

Jones, M. S., & Jones, O. T. G. (1969) *Biochem. J. 113*, 507−514.

Karr, S. R., & Dailey, H. A. (1988) *Biochem. J. 254*, 799−803.

Kim, Y. M., Bergonia, H. A., Muller, C., Pitt, B. R., Watkins, W. D., & Lancaster, J. R., Jr. (1995) *J. Biol. Chem. 270*, 5710−5713.

Labbe-Bois, R. (1990) *J. Biol. Chem. 265*, 7278−7283.

Lee, M., Arosio, P., Cozzi, A., & Chasteen, N. D. (1994) *Biochemistry 33*, 3679−3687.

Lepoivre, M., Flaman, J.-M., Bobé, P., Lemaire, G., & Henry, Y. (1994) *J. Biol. Chem. 269*, 21891−21897.

Miyamoto, K., Nakahigashi, K., Nishimura, K., & Inokuchi, H. (1991) *J. Mol. Biol. 219*, 393−398.

Miyamoto, K., Tanaka, R., Teramoto, H., Masuda, T., Tsuji, H., & Inokuchi, H. (1994) *Plant Physiol. 105*, 769−770.

Nakahashi, Y., Taketani, S., Okuda, M., Inoue, K., & Tokunaga, R. (1990) *Biochem. Biophys. Res. Commun. 173*, 748−755.

Nunoshiba, T., Derojas-Walker, T., Tannenbaum, S. R., & Demple, B. (1995) *Infect. Immun. 63*, 794−798.

Nussler, A. K., & Billiar, T. R. (1993) *J. Leukocyte Biol. 54*, 171−178.

Oria, R., Sanchez, L., Houston, T., Hentze, M. W., Liew, F. Y., & Brock, J. H. (1995) *Blood 85*, 2962−2966.

Pantopoulos, K., & Hentze, M. W. (1995) *Proc. Natl. Acad. Sci. U.S.A. 92*, 1267−1271.

Sassa, S., Granick, J. C., Eisen, H., & Ostertag, W. (1978) in *In Vitro Aspects of Erythropoiesis*, pp 268−270, Springer-Verlag, New York.

Smith, A. (1990) in *Biosynthesis of Heme and Chlorophylls* (Dailey, H. A., Ed.) pp 435−490, McGraw-Hill, New York.

Smith, A. G., Santana, M. A., Wallace-Cook, A. D. M., Roper, J. M., & Labbe-Bois, R. (1994) *J. Biol. Chem. 269*, 13405−13413.

Takahashi, Y., Hase, T., Wada, K., & Matsubara, H. (1983) *Plant Cell Physiol. 24*, 189−198.

Taketani, S., Nakahashi, Y., Osumi, T., & Tokunaga, R. (1990) *J. Biol. Chem. 265*, 19377−19380.

Weinberg, E. D. (1971) *J. Infect. Dis. 124*, 401−410.

Weiss, G., Werner-Felmayer, Werner, E. R., Grunewald, K., Wachter, H., & Hentze, M. W. (1994) *J. Exp. Med. 180*, 969−976.

BI952631P